

Simple process to nanostructured Raney-nickel electrodes for highly active and cost-efficient hydrogen evolution in alkaline water electrolysis (AWE)

Timon Günther, Jonas Schick, Timo Körner, Tobias Mangold, Richard Wehrich

Angaben zur Veröffentlichung / Publication details:

Günther, Timon, Jonas Schick, Timo Körner, Tobias Mangold, and Richard Wehrich. 2025. "Simple process to nanostructured Raney-nickel electrodes for highly active and cost-efficient hydrogen evolution in alkaline water electrolysis (AWE)." *International Journal of Hydrogen Energy* 136: 1124–30.
<https://doi.org/10.1016/j.ijhydene.2025.02.398>.

Nutzungsbedingungen / Terms of use:

CC BY 4.0

Dieses Dokument wird unter folgenden Bedingungen zur Verfügung gestellt: / This document is made available under these conditions:

CC-BY 4.0: Creative Commons: Namensnennung

Weitere Informationen finden Sie unter: / For more information see:

<https://creativecommons.org/licenses/by/4.0/deed.de>





Simple process to nanostructured Raney-nickel electrodes for highly active and cost-efficient hydrogen evolution in alkaline water electrolysis (AWE)

Timon Günther^{a,*}, Jonas Schick^a, Timo Körner^b, Tobias Mangold^c, Richard Wehrich^a

^a Chemistry of Materials and Resources, Department of Resource and Chemical Engineering, Institute for Materials Resource Management, University of Augsburg, Am Technologiezentrum 8, 86159, Augsburg, Germany

^b Anwenderzentrum Material- und Umweltforschung, Universitätsstr. 1a, 86159, Augsburg, Germany

^c Oberland Mangold GmbH, In der Enz 1, 82438, Eschenlohe, Germany

ARTICLE INFO

Handling Editor: Ibrahim Dincer

Keywords:

Water electrolysis
Hydrogen evolution
Raney nickel
Electrocatalysis
Nanostructured electrode

ABSTRACT

In this work we present a nanostructured nickel-based electrode with high surface area as cathode for the hydrogen evolution (HER) during alkaline water electrolysis (AEL). The electrodes are prepared via mechanical plating of aluminum on a nickel sheet and thermal treatment in N₂-atmosphere at different temperatures to achieve leachable NiAl-phases such as Ni₂Al₃ and NiAl₃. Focus is to increase the electrochemical surface area (ECSA) significantly. The electrochemical performance is evaluated with cyclic voltammetry (CV) and chronopotentiometry (CP) in a three-electrode and full cell setup at current densities up to 1 A/cm². High efficiency values at the cathode with Tafel slopes from 70 to 80 mV/dec and low overpotentials of 170–200 mV at high currents are determined. Electrochemical impedance spectroscopy (EIS) and chronopotentiometry (CP) are used to study resistances, degradation and stability of the fabricated electrodes. The “carpet-like” structure of the electrode leads to a 4200x increased surface area of the Nickel catalyst with optimized gas desorption and transport of hydrogen.

1. Introduction

Hydrogen is seen as sustainable fuel to replace fossil energy sources like oil and gas. High quantities of hydrogen can be produced by the combination of solar and wind energy with use of electrolyzers. Main challenges in the ongoing improvement concern the electrodes in terms of electrochemical efficiency and use of resources. Recent development in the field of hydrogen production took a lot of effort to produce cost-efficient and high-performing cell stacks. While proton exchange membrane (PEM) systems can currently reach current densities of >2 A/cm² and are useful to fluctuating electricity production and load changes with a fast ramp up, the PEM is dealing with problems like utilization of Platinum group metals (PGM) as catalysts. For cathodes and anodes Iridium, Platinum or Ruthenium are used leading up to 25% of the total electrolyzer costs [1–5]. Alkaline electrolysis (AEL) systems or recent studied anion exchange membrane (AEM) systems can overcome the use of PGMs due to the less corrosive alkaline media and application of Ni-based and highly structured electrodes [6]. This allows the application of low-cost electrodes and other components of the stack. Currently

most effort in the field of alkaline water electrolysis is made in research of various coatings with highly active and stable catalyst materials (e.g. Nickel, Iron, Cobalt or Copper), partially alloyed with Pt, Ru and Ir or in doped states [3,7]. Excellent performance during the hydrogen evolution reaction (HER) show galvanic coatings like Nickel–Molybdenum (Ni–Mo), plasma-sprayed Raney Nickel, Nickel foams or Iron-coated electrodes [5,8–10]. Low overpotentials between 240 and 420 mV with currents densities up to 1 A/cm² can be achieved according to López-Fernández et al. (2020) and Gannon et al. (2019) [9,10]. An alternative focus on (nano) structured electrodes is shown by works of Zhang et al. (2020) and Lee et al. (2022) designing gradual porosities or grooved electrodes to enhance fluid kinetics (KOH, H₂ or O₂) and desorption within the Tafel and Heyrowski-steps with surface structures that lead to higher availability of active sites of the catalyst material [2, 11,12]. Also catalyst coated diaphragms (CCD) are considered to be used for AEL applications without using a metal substrate [13]. Not only active coatings and high catalytic activity determine the efficiency of alkaline electrolyzers. The effect of hydrogen bubbles and adapted electrolyte flow cumulate to the overpotential during the hydrogen

This article is part of a special issue entitled: ANM2024 (Titus) published in International Journal of Hydrogen Energy.

* Corresponding author. Institute of Materials Resource Management (MRM), University of Augsburg, Am Technologiezentrum 8, D-86159, Augsburg, Germany.

E-mail address: timon.guenther@uni-a.de (T. Günther).

<https://doi.org/10.1016/j.ijhydene.2025.02.398>

Received 10 December 2024; Received in revised form 31 January 2025; Accepted 25 February 2025

Available online 2 March 2025

0360-3199/© 2025 The Authors. Published by Elsevier Ltd on behalf of Hydrogen Energy Publications LLC. This is an open access article under the CC BY license (<http://creativecommons.org/licenses/by/4.0/>).

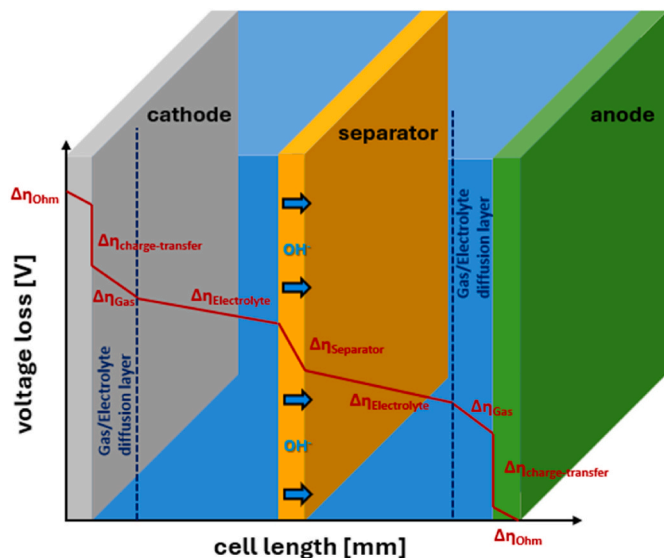


Fig. 1. Voltage loss in cross section of an electrolysis cell [2,3].

production [14–16]. Zhu et al. (2024) showed in their work the potential of Raney catalysts at current densities up to 1 A/cm² and higher [17]. With focus on PGM-free Raney-Nickel electrodes Tanaka et al. (2000) already reported the unleachability of Ni, Ni₃Al and NiAl in alkaline media [18]. Thus, this thermal step is modified in this work to form preferably leachable binary phases such as NiAl₃ or Ni₂Al₃ [5,18]. Thereby, the Aluminum content should be higher than 58 % and the temperature above 462 °C to reach diffusion of Aluminum atoms into the Ni-bulk. The precipitation of the catalytically inactive phase NiAl (1:1) during the heating should be avoided (see Fig. S1 in the supporting information (SI)) [3,19]. The selective leaching with KOH-solution of leachable Ni-phases allows to obtain high specific surface and porosity of the derived Ni-electrodes. To compare electrode performance, several processes at the surface of the electrodes and respective methods of measurements have to be taken into account, that are described subsequently.

1.1. Hydrogen evolution reaction (HER)

The hydrogen evolution at the cathode is characterized by three consecutive steps. In the Volmer-step as shown in formula 1 protons collect electrons to form atomic hydrogen which adsorbs at the catalyst surface [10]. Next, the Heyrovsky-step (formula 2) combines reduction of the hydrogen atoms from the Volmer-step and desorption of the H_{ad}-Atoms from the electrode surface to form molecular hydrogen [20, 21]. Molecular hydrogen is formed after desorption and combination of adsorbed H_{ad}-Atoms in the Tafel-step (see formula 3) [22]. The fugitive gas will be taken from the system and stored for further use [23–25].

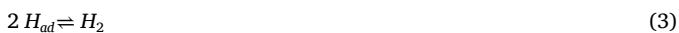
Volmer-step:



Heyrovsky – step:



Tafel – step:



1.2. Overpotential

The overpotential (or overvoltage) is the difference between the theoretical necessary cell voltage of 1.23 V and the applied cell potential for water splitting (>1.5 V). It is one of the most important parameters to

evaluate the overall performance of water electrolyzers or the performance of the catalyst at the electrode (formula 4). There are several methods to measure the overpotential at which either the oxygen evolution reaction (OER) or HER are carried out at a specific current density. Typically, cyclic voltammograms (CV) or linear sweep voltammetry (LSV) are potentiometric techniques which are used in the reaction region of the HER (<0.0 V vs. RHE) [19]. Scan rates from 5 to 20 mV/s are applied and iR-compensation is used to reduce the capacitive current during the measurement. With increasing current density, the overpotential increases due to the cumulation of electrical resistances of the electrolyte and membrane, charge transfer, mass transfer (e.g. high gas evolution) and slow desorption from the electrode surface which can result in a diffusion limitation and inefficient kinetics in the cell or electrolyzer system (formula 5). Fig. 1 shows the voltage loss in cross section of an electrolysis cell from cathode to anode and cumulation of each resistance [7,19].

$$E_{corrected} = E_{measured} - iR_{cumulated,system} \quad (4)$$

$$\Delta\eta_{Ges} = \Delta\eta_{Ohm} + \Delta\eta_{charge-transfer} + \Delta\eta_{Gas} + \Delta\eta_{Electrolyte} + \Delta\eta_{Separator} \quad (5)$$

1.3. Electrochemical surface area (ECSA)

The higher the amount of active sites on the surface of an electrode, the faster the reaction and higher the efficiency. This electrochemical active surface area (ECSA) can be determined by cyclic voltammetry (CV) using low to high scan rates [15]. Hereby the ECSA of electrodes can be determined by cyclic voltammetry around the open circuit potential (OCP) at ± 50 –100 mV. By charging and discharging the electrode double layer the charge of the double layer C_{DL} of each sample is measured. Using the same protocol for a Ni-bulk substrate the charge of the reference material C_{Ref} e.g. Ni-plate is needed to calculate the overall ECSA with this method. The charge of the double layer is resulting from the slope of the U–I-plot of the scan rate (mV/s) over the current (mA). The ECSA is calculated as follows in formula 6.

$$A_{ECSA} = \frac{C_{DL}}{C_{Ref}} \cdot A_{geo} \quad (6)$$

For the detection of the surface of electrodes other methods like H_{UPD} or CO-stripping after adsorption can be useful how Lukaszewski et al. (2016) showed for noble metal catalysts like polycrystalline Pt [19,26].

2. Material and methods

This work is focusing on the development of a cost-efficient and scalable manufacturing method leading to very high and active surfaces on Nickel-based electrodes through a pyrometallurgic and Raney-based method by Aluminum plated on a Nickel substrate [3].

2.1. Electrode preparation

The aim of the novel procedure is to prepare nanostructured Nickel electrodes that are thermally and structurally stable, highly porous and catalytically active after the leaching process. The electrodes are prepared from a nickel foil of 100 μm which is plated with aluminum foil with a thickness of 80 μm with up to 5–10 GPa in a rolling process. Celko et al. (2010) reported optimal diffusion of NiAl₃-phases near the eutectic melting point of 639.9 °C. Depending on the cooling rate used the phase morphology and formation can be significantly different [27]. The heating process of the highly pure (>99,9 %) bulk materials therefor was carried out in a furnace under N₂-atmosphere at temperatures, between the sintering and melting temperature of Aluminum at 600, 650, 700 and 750 °C for 1 h named NiAl600, NiAl 650, NiAl700 and NiAl750. The heating rate was set to 20 K/min and 10 K/min cooling rate back to room temperature. The overall reaction of the activation of Raney-Nickel was conducted as shown in formula 7:

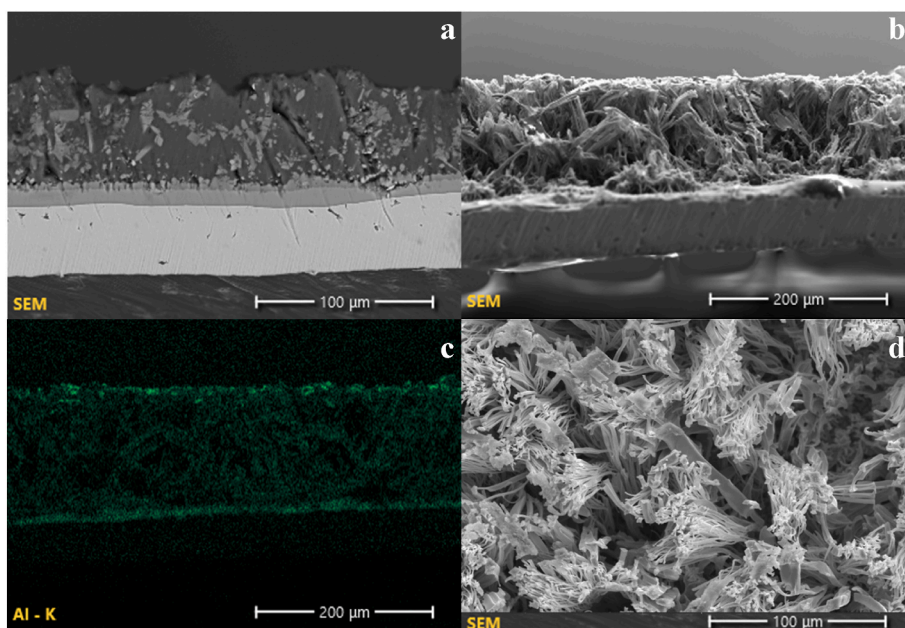
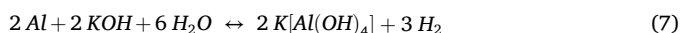


Fig. 2. SEM-images of the nano-structured Nickel electrode at 700 °C before (a) and after leaching (b) in 32 wt.-% KOH, cross-section, EDX-Mapping of remaining Al-content in cross-section (c) and SEM-image at top view after leaching (d).



The aqueous solution of potassium hydroxide (1.8 M) and potassium/sodium tartrate (1.5 M) was freshly prepared for each application to leach the samples. According to the procedure of Bernäcker et al. (2019), the leaching of Raney nickel takes place in two steps [9]. First, the samples are placed in the solution at 25 °C for 10–12 h. After the time has elapsed, the solution is replaced with a new batch. In the second step, the samples are leached at 80 °C for 2–4 h until hydrogen evolution stops. Remaining is a porous nickel structure which, depending on the starting alloy, form a highly porous structure or leading to cracks caused by shrinkage during cooling to freeze the leachable phases. Due to its pyrophoric character, Raney nickel should always be stored under water or ethanol according to Delannay et al. (1982) [28]. Commercial Ni-foam (Alantum Europe GmbH) and Ni-expanded metal (Sorst Streckmetall GmbH) was used as reference for the electrochemical measurements. The NiAl-sample at 750 °C showed almost no measurable hydrogen evolution during the leaching procedure. A formation of leachable phases such as NiAl₃ or Ni₂Al₃ is not reached and unleachable NiAl (1:1)- or Ni₅Al₃ (5:3)-phases dominate (see Fig. S1). The NiAl750 sample and higher temperatures prepared with this process were therefor excluded from further measurements. The PGM-samples (Pt–Ni) were prepared according to Ma et al. (2021) to add a further reference. [7].

2.2. Material characterization

2.2.1. Scanning electron microscopy (SEM-EDX)

Scanning electron microscope images were taken on a Prisma E-SEM with a Schottky field emission cathode of a tungsten single crystal (Thermo Fisher Scientific Inc.) at an accelerating voltage of 10–20 kV. For the topological characterization of the electrode surfaces and cross sections, the secondary electrons were analysed using a secondary electron detector (SE) as well as an angular backscatter-detector (ABS) at 100–1000× magnification. The beam width was dimensioned as 2·10⁻¹⁰ to 6·10⁻¹¹ mm. The Nickel electrodes were held in ethanol to avoid oxidation and then attached to a conductive carbon mat and placed on the sample holder [28]. Fig. 2a and b show SEM-images of a NiAl700 sample before and after the leaching process. A Ni-bulk with a thickness of 70–120 μm is found with a mesoporous 20 μm thick

structure between the bulk followed by Ni-wires with a thickness of 100 nm to 5 μm and length of up to 150 μm growing out of the dense Ni-bulk to form a carpet-like Ni-structure with high surface (Fig. 2d). The EDX-mapping of the cross section of the unleached electrode shows an Aluminum content of 48–52 wt.-% before and 1–3 wt.-% Aluminum remaining in NiAl and Ni₃Al after leaching of the fabricated electrode (Fig. 2c). For the NiAl600 and -650 the remaining Al-content varies between 5 and 8 wt% Al, so a higher amount of unleachable phases. More SEM-images and EDX-data in Table S1 and Figs. S2–5 in the supporting information.

2.2.2. Brunauer-Emmett-Teller (BET)

To support the electrochemical surface determination (ECSA), a BET gas adsorption measurement was carried out on leached electrodes to determine the real surface area quantitatively. The Nova-2200 (Quantachrome Instruments) was used for this purpose in a 4-point BET measurement with liquid nitrogen (T_{N2} = 77 K, p = 101.3 kPa) as the adsorbate [29]. A specific surface area of 10.91 m²/g was determined which results in a 4200x increased surface compared to an unstructured Ni-plate. The R² value for the BET-measurements was 0,9999 (Fig. S6, Table S2).

2.2.3. Compression tests

The compression test was performed at a Zwick Z5.0 (Zwick Roell Co., Germany) using a feed rate of 0.2 mm/min to observe mechanical stability of the leached electrodes. Here a compression of 17, 19.4 and 22.9 % for the NiAl600, NiAl 650, NiAl700 at 1 MPa (Fig. S7) is observed. Commercial Nickel foam showed a compression of 8.4 %. Deformation of the electrodes was reached above 1 MPa. Here only the foam showed distinct linear-elastic behavior. Similar results were shown by Barzergar et al. [30].

2.3. Electrochemical characterization

2.3.1. Three electrode setup

For the electrochemical measurements a three-electrode setup (Figs. S8–9) was used consisting of the developed electrodes, Pt wire and a reversible hydrogen electrode (Hydroflex©) were used as working electrode, counter electrode and reference electrode, respectively.

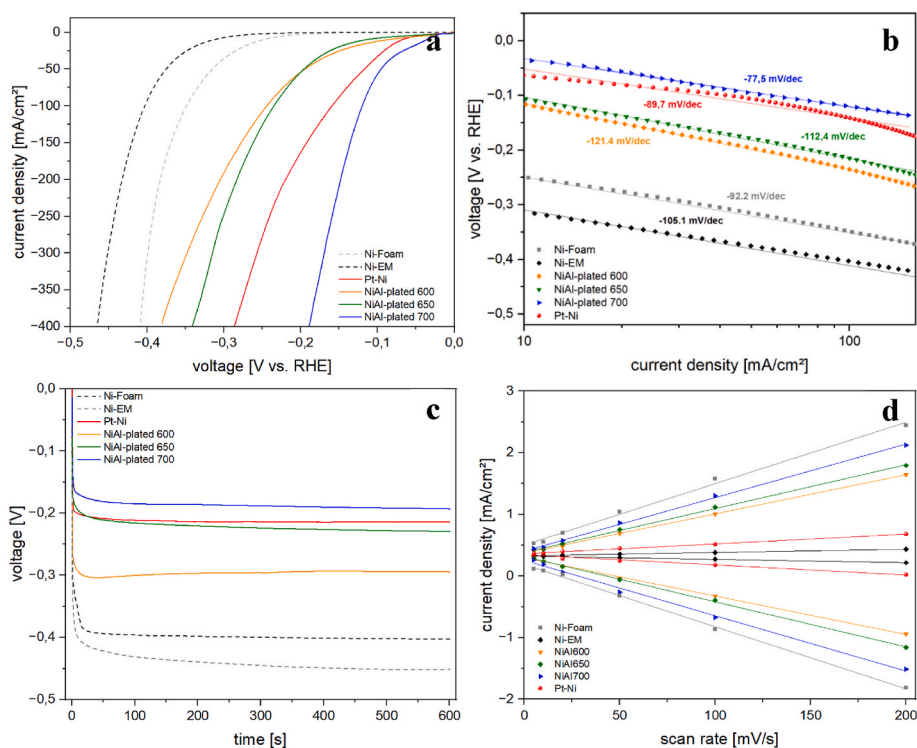


Fig. 3. Electrocatalytic properties in three-electrode setup during the HER in 32 wt.-% KOH, 10 mV/s scan rate, iR-compensated a) HER-activity of Raney-electrodes; b) Tafel-plots of the Raney-electrodes in the HER-range under various current densities; c) chronopotentiometric measurements at -100 mA/cm^2 ; d) Cyclic voltammograms (CV) $\pm 50 \text{ mV}$ around the OCP of the NiAl700 sample to determine the C_{DL} and ECSA, various scan rates.

Electrolyte was a 32 wt.-% KOH-solution. The temperature of the water bath with ultra-pure water (Milli-Q, $18.2 \text{ M}\Omega\text{cm}$) saturated with N_2 was kept at room temperature ($20\text{--}25 \text{ }^\circ\text{C}$). The temperature was measured with a K-type thermocouple [31,32].

A potentiostat VSP-300 (Biologic) with a 10 A booster was used. The separator is a UTP 500 from Agfa consisting of an open mesh polyphenylene sulfide fabric which is coated with a mixture of a polymer and zirconium oxide. The ionic resistance at a temperature of $25\text{--}90 \text{ }^\circ\text{C}$ in 10 % KOH electrolyte is between 0.25 and $0.44 \text{ }\Omega/\text{cm}^2$, while at 32 wt.-% KOH the resistance differs from 0.1 to $0.27 \text{ }\Omega/\text{cm}^2$ [33].

A cleaning cycle (CV-pretreatment) is applied by potential cycling between 1.2 and 1.6 V vs. RHE at a scan rate of 200 mV/s to remove adsorbed H-species until a stable cyclic voltammogram is found ($\approx 30\text{--}50$ cycles). Followed by a ZIR-measurement to measure specific resistances at 10 kHz for 85% iR-compensation at each measurement. The cyclic voltammograms (forward scans as shown in Fig. 3a) were recorded at a scan rate of 10 mV/s [31], in a voltage range from 0.0 to -0.4 V vs. RHE to evaluate the HER-activity. For the detection of the ECSA, CV's around OCP $\pm 50 \text{ mV}$ with $5\text{--}200 \text{ mV/s}$ scan rate are applied. Chronopotentiometric measurements were performed at -100 mA/cm^2 for 10 min to observe the quasi-stationary behavior of the electrodes during polarization in the HER-region. Impedance measurements (EIS) were performed to observe the specific resistances at alternating current with a scanning frequency from 5 mHz to 500 kHz . The determination of the electrochemical active surface area (ECSA) is used to support the BET-results via physisorption with the electrochemical response during the hydrogen evolution. Therefore, CVs with different scan rates from 10 to 200 mV/s are carried out in a potential region from $\pm 50 \text{ mV}$ around the open circuit voltage (OCV). Before each CV-step an OCP-determination and a ZIR for iR-compensation was carried out to avoid capacitive effects during the measurement. In this work, the value of the C_s is estimated to be $4.0 \cdot 10^{-5} \text{ F cm}^{-2}$ [7,26,32].

2.3.2. Full cell setup

The fabricated electrodes were tested in a single cell (Redox Flow[®]) with an active area of 9 cm^2 ($3 \times 3 \text{ cm}$) between two stainless steel endplates separated by an Agfa Zirfon UTP 500 separator (Fig. S10) [5]. Nickel expanded mesh (Sorst Streckmetall GmbH) was used as anode. All fabricated electrodes were leached after cell assembly. The cell was sealed using two PTFE gaskets with a thickness of $250 \text{ }\mu\text{m}$. The temperature was controlled in both anodic and cathodic electrolyte reservoirs to heat the electrolyte and the cell to $70 \text{ }^\circ\text{C}$, all integrated in an in-house built test station. As potentiostat a VSP-300 (Biologic) with a 10 A booster was used.

After heating the cell the open circuit voltage is measured for $1\text{--}2 \text{ h}$ until it is stabilized. Current steps at $100, 200, 300, 400, 500, 600, 700, 800, 900$ and 1000 mA/cm^2 are applied for 10 min each to detect corresponding voltages. Followed by a long-term measurement at 700 mA/cm^2 for 150 h. Here an altered NiAl700 sample with lifetime of 500 h was used to estimate the long-term durability of the best performing electrode [34].

3. Results and discussion

3.1. Electrocatalytic activity of surface structured Ni-electrodes – three electrode setup

The catalytic activity with polarization of the electrodes in the HER-region shows strong dependency on temperature during the heating and formation of leachable phases. Best performance was found for the samples prepared at $700 \text{ }^\circ\text{C}$ (NiAl700) with an overpotential of $150\text{--}200 \text{ mV}$ at current densities of -200 to -400 mA/cm^2 (Fig. 3a). The Tafel slope performance shows a measured value of -77.5 mV/dec better than commercially used PGM-catalysts applied on Nickel substrates with -89.7 mV/dec as shown in Fig. 3b [7]. Lower annealing temperatures of 650 and $600 \text{ }^\circ\text{C}$ show overpotentials of $280\text{--}350$ and $300\text{--}370 \text{ mV}$ at comparable current densities. With a Tafel-performance of -121.4 and

Table 1
Electrochemical characteristics of the examined electrodes in 32 wt.-% KOH.

Electrode	Overpotential at −100 mA/cm ² vs. RHE [mV]	Tafel slope [mV/dec]	Electrochemical active surface area [m ² /g]
Ni-foam	402	92.2	12.52
Ni-expanded mesh	451	105.1	0.31
Ra-Ni [14,17,35, 36]	220–330	70–120	–
Electrodeposited Ni [37]	190–280	105–125	–
Pt–Ni	214	89.7	4.16
NiAl600	294	121.4	7.82
NiAl650	229	112.4	8.81
NiAl700	192	77.5	9.19

−112.4 mV/dec those electrodes are only suitable at lower current densities compared to commercially available Ni-Foam and Ni-expanded mesh (Fig. 3d). The quasi-stationary activity of the electrodes in Fig. 3c at −100 mA/cm² proof the results from the CV-measurements showing best performance in the NiAl700 sample with −190 mV vs. RHE followed by the Pt–Ni reference and NiAl650 sample at 214 and 229 mV at constant current. Expanded mesh, Ni-Foam and the NiAl600 sample show with 451, 402 and 294 mV much higher overpotentials.

Highest determined ECSA values for the Ni foam are 12.52 m²/g. The higher overpotential values proof limited diffusion of hydrogen through the electrode structure, whereas the plated samples have an ECSA of 7.8–9.2 m²/g but 170–210 mV lower potential. BET measurements show a value of 10.91 m²/g for the NiAl700. The correlation from the ECSA to the overpotential relies not only on the surface area but also surface structure as results in Table 1 show. Plated samples refer to a gradient electrode structure to improve hydrogen bubble transport and faster desorption to enhance the overall kinetics whereas Ni-foam shows a non-gradient pore structure in which the kinetics a transport of hydrogen at high current-densities is limited. NiAl600 and NiAl650 electrodes show a similar effect due to a non-carpet-like structure which would enhance the kinetics during hydrogen evolution like with the NiAl700 sample. Recent studied Raney-electrodes reach an

overpotential of 220–330 mV at −100 mA/cm² with a tafel slope of 70–120 mV/dec as shown in Table 1 [14,17,35,36].

3.2. Full cell

The performance of the electrodes in the full cell at various current densities support the results in the three-electrode measurements. The plated electrodes at 600, 650 and 700 °C show increasing efficiency with higher tempering temperature. Best performance is found for the NiAl700 sample with 1.81 V (1.84 V altered) at 500 mA/cm² and 1.87 V (1.90 V altered) at 1 A/cm² followed by the NiAl650-sample with 1.97 and 2.03 V (Fig. 4a). Commercial Ni-Foam and Ni-EM with 2.3 V and 2.46 V at 1 A/cm² show higher overpotentials. A best performance value of 1.71–1.79 V was reported by Zhu et al. (2024) with nanodendritic Raney-Nickel used as cathode and NiFeOH as anode catalyst [17]. Correlating overpotentials for a typical operating condition of 700 mA/cm² are shown in Fig. 4b. Ni-Foam and Ni-EM show overpotentials of 790–880 mV which corresponds to a voltage efficiency of 62–66 %. Nanostructured electrodes increase the kinetics at the cathode side and can reach overpotentials of 500 mV–730 mV, resulting in voltage efficiencies of 78–84 %. Long-term measurements at 700 mA/cm² are performed for Ni-foam, unaltered and altered NiAl700 electrodes for 150 h (Fig. 4c). Ni-Foam shows a degradation rate of 142.7 μV/h at a cell voltage of 2.17–2.24 V at corresponding current density. New and 500 h altered NiAl700-samples (see Fig. S11 in the supporting information) samples show an average degradation rate of 24.7 and 33.2 μV/h with voltages of 1.73 and 1.78 V. Impedance spectroscopy measurements (EIS) of the NiAl700 electrode show hydrogen production starting at 1.5 V with decreasing resistances during the charge transfer and conductive electrode structure. Due to high gas production the reaction at currents is kinetically limited. This has an impact on the cell resistance due to overpotential of the higher charge transfer and gas diffusion barrier. Between 1.7 and 1.9 V the cell resistance is in a range from 9 to 20 mΩcm as presented in Fig. 4d. This shows that even at higher voltage and corresponding high current densities of >1 A/cm² exhibit low area specific resistances and overpotentials allow a much faster and efficient hydrogen production at the cathode.

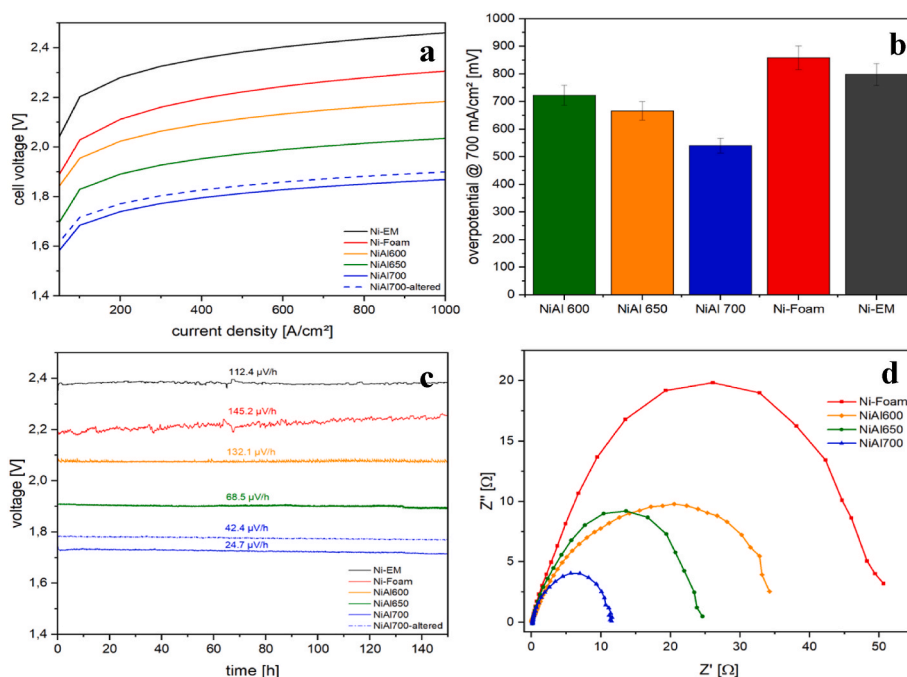


Fig. 4. Full cell performance of the electrodes at 32 wt.-% KOH, UTP 500 separator, Nickel expanded mesh is used as anode, a) voltage performance, sample at 1.3–1.9 V, b) overpotential of the electrodes, c) long-term test at 700 mA/cm², d) electrochemical impedance spectra of NiAl600, NiAl650, NiAl700 and Ni-foam.

4. Conclusion

Raney-based Nickel-electrodes for alkaline water electrolysis were prepared by a novel method. From Ni-electrodes were obtained via plating and thermal treatment leading to a moderate to excellent electrochemical performance. Current densities up to 1 A/cm² show low overpotentials at the cathode. Excellent tafel slope performance for the NiAl700 can be reached. Mid-term measurements up to 150 h confirm slow degradation and good stability of the fabricated electrodes and capability for further ageing tests and industrialization. Crucial is the heating temperature of the electrode, preferably above 650 °C. Here leachable phases like Ni₂Al₃- and NiAl₃ are formed at the interface of plated Ni and Al. Temperatures higher than 700 °C should be avoided due to unactive NiAl-phase development and remaining Al-content after activation. This high surface area is crucial to overcome issues lowering the hydrogen output like gas bubbling and surface attachment on active sites of the electrodes during Tafel and Heyrowski step. The gradual structure of the manufactured electrodes leads to an increased reaction kinetics during the HER and allows optimized hydrogen gas detaching active centers of the catalytically active Nickel sites. Fast gas desorption and transport of hydrogen at high currents without blocking inner pore structures of the electrode f.e. with Ni-foam is reached. The groups of Peng, Zhang and Lee demonstrated the potential of surface structured electrodes in their previous works [2,11,12]. A measurement protocol of >1000 h should be considered in the next step to show electrode degradation over longer terms. Next to classic long-term measurements the authors are working on the development of accelerated stress tests (AST's) to enhance the degradation artificially. Further mechanistic studies should be performed especially when higher compression in a zero-gap design is applied. Nanostructured electrodes are an alternative to classical surface coatings and enhance the reaction mechanisms during the HER to make AEL-systems cost-efficient, reduce investment and operating costs (CAPEX/OPEX) and to substitute PGM-catalysts. To reach the IRENA goals of >2 A/cm² at < 1.7 V until 2050, here a first step is made.

CRedit authorship contribution statement

Timon Günther: Writing – review & editing, Writing – original draft, Visualization, Project administration, Methodology, Formal analysis, Data curation, Conceptualization. **Jonas Schick:** Writing – review & editing, Visualization, Software, Methodology, Data curation. **Timo Körner:** Writing – review & editing, Supervision, Resources, Project administration, Funding acquisition, Formal analysis. **Tobias Mangold:** Writing – review & editing, Supervision, Resources, Project administration, Funding acquisition. **Richard Weihrich:** Writing – review & editing, Validation, Supervision, Resources, Project administration, Funding acquisition.

Declaration of competing interest

The authors declare that they have no known competing financial interests or personal relationships that could have appeared to influence the work reported in this paper.

Acknowledgements

The authors would like to thank the Bavarian State Ministry of Economic Affairs, Regional Development and Energy for the financial support of our studies in the field of alkaline water electrolysis. Additionally, the Elitenetzwerk Bayern in the program of “macromolecular science” supported the authors work. Further we like to thank Stefan Schmitt for supporting the mechanical testing of the electrodes.

Appendix A. Supplementary data

Supplementary data to this article can be found online at <https://doi.org/10.1016/j.ijhydene.2025.02.398>.

References

- [1] Strmcnik D, Lopes PP, Genorio B, Stamenkovic VR, Markovic NM. Design principles for hydrogen evolution reaction catalyst materials. *Nano Energy* 2016;29:29–36.
- [2] Lee C, Kort-Kamp WJM, Yu H, Cullen DA, Patterson BM, Arman TA, Komini Babu S, Mukundan R, Borup RL, Spendlow JS. Grooved electrodes for high-power-density fuel cells. *Nat Energy* 2023;8:685–94.
- [3] Hoang AL, Balakrishnan S, Hodges A, Tsekouras G, Al-Musawi A, Wagner K, Lee C-Y, Swiegers GF, Wallace GG. High-performing catalysts for energy-efficient commercial alkaline water electrolysis. *Sustain Energy Fuels* 2022;7:31–60.
- [4] Sharshir SW, Joseph A, Elsayad MM, Tareemi AA, Kandeal AW, Elkadeem MR. A review of recent advances in alkaline electrolyzer for green hydrogen production: performance improvement and applications. *Int J Hydrogen Energy* 2024;49:458–88.
- [5] Karacan C, Lohmann-Richters FP, Shviro M, Keeley GP, Müller M, Carmo M, Stolten D. Fabrication of high performing and durable nickel-based catalyst coated diaphragms for alkaline water electrolyzers. *J Electrochem Soc* 2022;169:54502.
- [6] Yang B, Zhang R, Shao Z, Zhang C. The economic analysis for hydrogen production cost towards electrolyzer technologies: current and future competitiveness. *Int J Hydrogen Energy* 2023;48:13767–79.
- [7] Ma Z, Chen C, Cui X, Zeng L, Wang L, Jiang W, Shi J. Hydrogen evolution/oxidation electrocatalysts by the self-activation of amorphous Platinum. *ACS Appl Mater Interfaces* 2021;13:44224–33.
- [8] Bao F, Kempainen E, Dorbandt I, Bors R, Xi F, Schlatmann R, van de Krol R, Calnan S. Understanding the hydrogen evolution reaction kinetics of electrodeposited nickel-molybdenum in acidic, near-neutral, and alkaline conditions. *Chemelectrochem* 2021;8:195–208.
- [9] Bernäcker CJ, Rauscher T, Büttner T, Kieback B, Röntzsch L. A powder metallurgy route to produce raney-nickel electrodes for alkaline water electrolysis. *J Electrochem Soc* 2019;166:F357–63.
- [10] Gannon WJ, Dunnill CW. Raney Nickel 2.0: development of a high-performance bifunctional electrocatalyst. *Electrochim Acta* 2019;322:134687.
- [11] Zhang Y, Liu T, Dong D, Jiang X, Deng C, Liu M. A novel nickel electrode with gradient porosity distribution for alkaline water splitting. *Int J Hydrogen Energy* 2020;45:24248–52.
- [12] Peng L, Yang N, Yang Y, Wang Q, Xie X, Sun-Waterhouse D, Shang L, Zhang T, Waterhouse GIN. Atomic cation-vacancy engineering of NiFe-layered double hydroxides for improved activity and stability towards the oxygen evolution reaction. *Angew Chem* 2021;60:24612–9.
- [13] Karacan C, Lohmann-Richters FP, Shviro M, Keeley GP, Müller M, Carmo M, Stolten D. Fabrication of high performing and durable nickel-based catalyst coated diaphragms for alkaline water electrolyzers. *J Electrochem Soc* 2022;169:54502.
- [14] Jensen VH, Moretti ER, Busk J, Christiansen EH, Skov SM, Jacobsen E, Kraglund MR, Bhowmik A, Kieback R. Machine learning guided development of high-performance nano-structured nickel electrodes for alkaline water electrolysis. *Appl Mater Today* 2023;35:102005.
- [15] Günther TE, Loukrakpam R, Gomes BF, Soisson A, Moos M, Nguyen BDL, Shah S, Roth C. Reliable testing of acidic OER catalysts in GDE half-cell set-up at industrially-relevant current densities. *Electrochim Acta* 2025;512:145474.
- [16] Cao X, Zhao N, Zhang S, Zhou L, Hu Y, Yun J. Investigation of the hydrogen bubble effect on the overpotential in an alkaline water electrolyzer. *Int J Hydrogen Energy* 2024;49:47–57.
- [17] Zhu Z, Lin Y, Fang P, Wang M, Zhu M, Zhang X, Liu J, Hu J, Xu X. Orderly nanodendritic nickel substitute for Raney nickel catalyst improving alkali water electrolyzer. *Adv Mater* 2024;36:e2307035.
- [18] Shin-ichi Tanaka, Norimitsu Hirose, Toshiyuki Tanaki, and Yukio H. Ogata, Effect of Ni-Al precursor alloy on the catalytic activity for a Raney-Ni cathode.
- [19] Wu L, He Y, Lei T, Nan B, Xu N, Zou J, Huang B, Liu CT. Characterization of porous Ni3Al electrode for hydrogen evolution in strong alkali solution. *Mater Chem Phys* 2013;141:553–61.
- [20] Rheinländer PJ, Herranz J, Durst J, Gasteiger HA. Kinetics of the hydrogen oxidation/evolution reaction on polycrystalline Platinum in alkaline electrolyte reaction order with respect to hydrogen pressure. *J Electrochem Soc* 2014;161:F1448–57.
- [21] Santos E, Hindelang P, Quaino P, Schmickler W. A model for the Heyrovsky reaction as the second step in hydrogen evolution. *Physical chemistry chemical physics PCCP* 2011;13:6992–7000.
- [22] Raja Sulaiman RR, Hanan A, Wong WY, Mohamad Yunus R, Shyuan Loh K, Walvekar R, Chaudhary V, Khalid M. Structurally modified MXenes-based catalysts for application in hydrogen evolution reaction: a review. *Catalysts* 2022;12:1576.
- [23] Carmo M, Fritz DL, Mergel J, Stolten D. A comprehensive review on PEM water electrolysis. *Int J Hydrogen Energy* 2013;38:4901–34.
- [24] Aricò AS, Siracusano S, Brigioglio N, Baglio V, Di Blasi A, Antonucci V. Polymer electrolyte membrane water electrolysis: status of technologies and potential applications in combination with renewable power sources. *J Appl Electrochem* 2013;2013:107–18.
- [25] Durst J. Hydrogen oxidation and evolution reaction kinetics on carbon supported Pt, Ir, Rh, and Pd electrocatalysts in acidic media. *J Electrochem Soc* 2015:F190.

- [26] Łukaszewski M, Soszko M, Czerwiński A. Electrochemical methods of real surface area determination of noble metal electrodes – an overview. *Int J Electrochem Sci* 2016;11:4442–69.
- [27] Čelko L, Klakurková L, Švejcár J. Diffusion in Al-Ni and Al-NiCr interfaces at moderate temperatures. *Defect Diffusion Forum* 2010:771–7.
- [28] Dellanay F, Damon JP, Masson J, Delmon B. Quantitative XPS-analysis of the surface composition of Raney nickel catalysts. *Appl Catal* 1982:169–80.
- [29] Liu X, Zhou Y, Zhou W, Li L, Huang S, Chen S. Biomass-derived nitrogen self-doped porous carbon as effective metal-free catalysts for oxygen reduction reaction. *Nanoscale* 2015;7:6136–42.
- [30] Barzegar F, Salehi A, Moloodi A. An investigation of the effect of sintering conditions on the mechanical behavior of electroplated nickel foams. *Metall Mater Trans B* 2019;50:1988–96.
- [31] López-Fernández E, Gil-Rostrá J, Espinós JP, González-Elipe AR, de Lucas Consuegra A, Yubero F. Chemistry and electrocatalytic activity of nanostructured nickel electrodes for water electrolysis. *ACS Catal* 2020;10:6159–70.
- [32] Liu Y, Liang X, Gu L, Zhang Y, Li G-D, Zou X, Chen J-S. Corrosion engineering towards efficient oxygen evolution electrodes with stable catalytic activity for over 6000 hours. *Nat Commun* 2018;9:2609.
- [33] Schalenbach Maximilian, Lueke Wiebke, Stolten Detlef. Hydrogen diffusivity and electrolyte permeability of the Zirfon PERL separator for alkaline water electrolysis. *J Electrochem Soc* 2016:1480–8.
- [34] Siracusano S, Hodnik N, Jovanovic P, Ruiz-Zepeda F, Šala M, Baglio V, Aricò AS. New insights into the stability of a high performance nanostructured catalyst for sustainable water electrolysis. *Nano Energy* 2017;40:618–32.
- [35] Han W-B, Kim I-S, Kim M, Cho WC, Kim S-K, Joo JH, Lee Y-W, Cho H-S, Kim C-H. Directly sputtered nickel electrodes for alkaline water electrolysis. *Electrochim Acta* 2021;386:138458.
- [36] Zhu Y, Liu T, Li L, Song S, Ding R. Nickel-based electrodes as catalysts for hydrogen evolution reaction in alkaline media. *Ionics* 2018;24:1121–7.
- [37] Harada Y, Hua Q, Harris LC, Yoshida T, Gewirth AA. Electrodeposition of fractal structured nickel for hydrogen evolution reaction in alkaline. *Chemelectrochem* 2024;11.